Clays and Clay Minerals, Vol. 48, No. 1, 75–84, 2000.

DIELECTRIC-RELAXATION SPECTROSCOPY OF KAOLINITE, MONTMORILLONITE, ALLOPHANE, AND IMOGOLITE UNDER MOIST CONDITIONS

TOMOYUKI ISHIDA,[1] TOMOYUKI MAKINO,[2] AND CHANGJUN WANG[1]

[1]Department of Agricultural Engineering, Kagawa University, Miki, Kagawa 761-0795, Japan
[2]Soil Chemistry Laboratory, National Institute of Agro-Environmental Sciences of Japan, Tsukuba, Ibaraki 305-8604, Japan

Abstract—The dielectric behavior of kaolinite, montmorillonite, allophane, and imogolite samples adjusted to a water potential of 33 kPa was examined using a time-domain reflectometry method over a wide frequency range of 10^3–10^{10} Hz. A dielectric relaxation peak owing to bound H_2O was observed. The observation of this peak required the precise determination of the contributions of dc conductivity. The peak is located at 10 MHz, indicating that the relaxation time of the bound H_2O is approximately ten times longer than the relaxation time of bound H_2O with organic polymers, such as an aqueous globular-protein solution. The structure of bound H_2O differs between phyllosilicates and amorphous phases, based on differences in relaxation strength and the pattern of distribution of the relaxation times. The dielectric process involving rotation of bulk H_2O molecules was also observed at 20 GHz. The relaxation strength of bulk H_2O increased with an increase in the water content. The interfacial polarization in the diffuse double layer occurred only in montmorillonite and kaolinite, indicating that mechanisms involving the Maxwell-Wagner and surface-polarization effects cannot be extended to include allophane and imogolite. Although these results suggest that additional work is required, a tentative conclusion is that a tangential migration of counter-ions along clay surfaces may be important.

Key Words—Allophane, Bound Water, Complex Permittivity, Dielectric-Relaxation Spectroscopy, Imogolite, Interfacial Polarization, Kaolinite, Montmorillonite, Time-Domain Reflectometry.

INTRODUCTION

Dielectric-relaxation spectroscopy probes a molecular environment on the broad time domain between 10^{-12}–10^{-2} s, compared with other methods, such as nuclear magnetic resonance (NMR) spectroscopy whose time scale is between 10^{-10}–10^{-3} s. Therefore, dielectric-relaxation spectroscopy provides data concerning many molecular arrangements of H_2O depending on the time scale involved (Sposito and Prost, 1982). In clay-mineral studies, dielectric measurements obtain information about the bound H_2O on clay surfaces (*e.g.,* Fripiat *et al.,* 1965; Mamy, 1968; Weiler and Chaussidon, 1968; Hoekstra and Doyle, 1971; Calvet, 1975; Hall and Rose, 1978) and about the interfacial region between clay particles (*e.g.,* Lockhart, 1980a, 1980b; Raythatha and Sen, 1986).

Mamy (1968) and Calvet (1975) performed dielectric measurements on one-layer hydrated montmorillonite by changing the temperature at a fixed frequency between 300 Hz and 10 kHz. They concluded that the rotational motions of bound H_2O on Na- and K-rich montmorillonite are on the same scale as those in free H_2O. On the other hand, the rotational times on the montmorillonite saturated with bivalent cations are comparable to ice (Sposito and Prost, 1982). The conclusion implies that the relaxation times of bound H_2O are separated by $\sim 10^5$ orders of magnitude, depending on the solvation complexes formed with the exchangeable cations. For an aqueous electrolyte solution, NMR data indicate that the rotational correlation times for H_2O molecules in the first hydration sphere around the cation might be different by no more than one order in magnitude between monovalent and bivalent cations (Hertz, 1973). In general, for isotropic motion, the NMR correlation time is more closely related to the dielectric-relaxation time because the latter is three times the former (*e.g.,* Carrington and McLachlan, 1967). Furthermore, the relation is applicable to the correlation time and the relaxation time for bound H_2O in biopolymer solutions (Fukuzaki *et al.,* 1992, 1995). The large difference in the dielectric-relaxation time probably cannot be explained by only the small difference owing to the solvation of exchangeable cations.

Hall and Rose (1978) measured dielectric-absorption curves for kaolinite at very low-water contents over the frequency range of 100 to 10 MHz. One absorption peak was found. The mechanism responsible for absorption was concluded to be caused by H_2O molecules bound to kaolinite. Judging from the values of the relaxation time, H_2O molecules in a one-layer hydrate have strong similarities to an "ice-like structure", the exchangeable cation is monovalent. These results are not consistent with those for montmorillonite (see above). Note, however, that there is evidence of another absorption found at near 10 MHz.

Lockhart (1980a, 1980b) obtained dielectric-dispersion curves for montmorillonite and kaolinite suspensions over the frequency range similar to that used by Hall and Rose. The suspensions varied between highly

dilute to thick. Only one relaxation process was attributed to polarization of the surface double layer. Because these results were not obtained at a high resolution of frequency, the relaxation process owing to bound H_2O could not be identified, even if the relaxation existed. Thus, bound H_2O on clay suspensions or moist clays was thought to be difficult to ascertain, because the solvent usually has a large dielectric constant and the relaxation strength of bound H_2O is thought too small to be observed.

Most of the previous results were obtained by measuring a narrow frequency range, especially low frequencies, or by changing the temperature at a fixed frequency. Therefore, these experimental conditions may limit the resulting conclusions. Previous results suggest that clay-water systems have multiple relaxation processes, such as interfacial polarizations around the clay particles and rotational relaxation of bound and free H_2O; therefore, the dielectric behavior is expected to be complicated. Useful and precise dielectric information may be obtained only when each relaxation process is extracted from the complicated overall behavior based on the measurement over wide frequency ranges and at high resolutions. Another problem is that the dielectric results from previous studies are restricted to very low-water contents. Because the physicochemical states of H_2O and counter-ions near the clay surfaces change with increasing water content, the dielectric results obtained at a low-water content may not be applicable to other water contents. Ishida and Makino (1999a, 1999b) showed that the dielectric properties of clay suspensions are different from those at very low-water contents. However, dielectric properties under moist conditions are not yet clarified.

Time-domain reflectometry (TDR) employed in the present study gives the complex permittivity continuously over a wide frequency domain (1 kHz to 20 GHz); therefore, it is easy to extract each relaxation process. In general, clay-water systems under moist conditions have a high dc conductivity. Hence, the contribution of dc conductivity to the complex permittivity must be precisely evaluated, especially in the low-frequency range. This evaluation is possible using a reference TDR method (Cole *et al.*, 1980; Mashimo *et al.*, 1987a). If a standard sample with known permittivity is employed as a reference and the conductivity is adjusted to be approximately the same as that of an unknown sample, the complex permittivity of the unknown sample can be obtained as a function of the ratio of the Fourier transforms of the two reflected waves from the known and the unknown samples, respectively.

In this study, the TDR method was used to investigate the dielectric properties of moist minerals. Our focus is on ascertaining the relaxation parameters of bound H_2O, especially the relaxation time. By using this method, bound H_2O was confirmed in biopolymers, such as DNA (Mashimo *et al.*, 1989), globular protein (Miura *et al.*, 1994), aqueous solutions, and moist collagen (Shinyashiki *et al.*, 1990). For moist collagen, the relaxation strength observed at 100 MHz depends on the water content and does not occur for dried collagen. Thus, this process is caused by the orientation of strongly bound H_2O to topocollagen. The relaxation strength at 100 MHz for the globular proteins is in proportion to the surface area of these proteins, suggesting that the relaxation process is caused by the orientation of bound H_2O molecules on the protein surface.

Our interest also relates to the mechanism responsible for a very large low-frequency relaxation process. Possible mechanisms include the Maxwell-Wagner effect and the surface-polarization effect. The former occurs in material composed of a layer of insulating material covered with a layer of conduction medium. Clay samples can be regarded as mixtures of a conduction medium (the water in all the different forms) and an insulating material (silicate layer of the clay mineral). The latter is ascribed to the net displacement of counter-ions as a result of the influence of an external electric field and hence is caused by deformation of the diffuse lining of the double layer. In deducing the boundary conditions of the Maxwell-Wagner polarization theory, the tangential flux of electrical charges is considered negligible in comparison with the normal flux because the space charge is very thin near the surface of the insulating material. However, the surface-polarization theory includes the tangential flux. The Maxwell-Wagner theory may not be correct if the particle surface carries a sufficiently high charge that the concentration of the counter-ions, and thus the conductivity in the diffuse part of the double layer, substantially exceeds the conductivity in the bulk (Dukhin, 1973).

Samples for study were kaolinite, montmorillonite, allophane, and imogolite. As far as we know, moist allophane and imogolite have not been studied by dielectric techniques. Since the water potential is an important property of clays for agriculture and civil engineering, dielectric measurements were performed for the sample whose concentration was controlled so that the water potentials of the four samples were kept the same.

MATERIALS AND METHODS

Sample preparation

The samples used here were kaolinite from Kagoshima Prefecture (Muraoka, 1951), montmorillonite from Yamagata Prefecture (Sueno and Nakaishi, 1992), allophane (Yoshinaga, 1966), and imogolite (Miyauchi and Aomine, 1966). For the montmorillonite and kaolinite samples, the size fraction of <2 μm was separated by sedimentation. After saturation with

https://doi.org/10.1346/CCMN.2000.0480110 Published online by Cambridge University Press

Na by washing five times with a 1 N solution of NaCl, the excess NaCl was removed by centrifugation and the samples were air-dried at room temperature. After oxidation of organic matter in the allophane sample with H_2O_2, the sample was successively treated with dithionite-citrate (Mehra and Jackson, 1960) and 2% Na_2CO_2 (Jackson, 1979). The size fraction of <2 μm was obtained from the suspension with a pH of 9. The allophane was Na saturated by following a similar method as used for montmorillonite and kaolinite. The sample was stored under moist conditions. The imogolite sample was prepared in the same way as allophane, except that the value of pH was 4. The samples were mixed with deionized and distilled water obtained from Wittaker Bioproducts, Inc. The water content of each sample was adjusted using a pressure-plate apparatus to a water potential of 33 kPa. The resultant water content, on the basis of 110°C oven drying, is: kaolinite, 74.5 wt. %; montmorillonite, 724.3 wt. %; allophane, 175.8 wt. %; imogolite, 2406 wt. %.

TDR method

Dielectric measurements in the frequency range of 1 kHz to 20 GHz were performed following the TDR method (Cole *et al.,* 1980; Mashimo *et al.,* 1987a). In this method, a step-voltage pulse, with a 30-ps rise time and 200-mV height, generated by a tunnel diode passes through a flexible coaxial cable (Suhner Electrics, Ltd., Sucoform 141PE, 50 Ω, dc: 26.5 GHz) to the sample surface upon which the applied pulse is reflected. The form of the reflected pulse is recorded and digitized by a digitizing oscilloscope (Hewlett Packard, HP54121T, dc: 20 GHz). The wave from was accumulated 128 times for each measurement. As derived by Cole (Cole, 1975a, 1975b; Cole *et al.,* 1980), the complex permittivity of unknown sample $\epsilon_x^*(\omega)$ where ω is the angular frequency is given by Equation (1) (see Table 1). A similar equation can be obtained for the sample of known permittivity $\epsilon_s^*(\omega)$ [see Equation (2) in Table 1]. Taking into account the elimination of $v_0(\omega)$, combining Equations (1) and (2) gives the estimation of $\epsilon_x^*(\omega)$ as a function of $\epsilon_s^*(\omega)$ [see Equation (3) in Table 1].

In this study, a dilute NaCl aqueous solution, which gives the same dc conductivity as the unknown sample, was used as a reference sample. The effects of NaCl concentration on the complex permittivity of water and on the dc conductivity are well known (Winsor and Cole, 1982a, 1982b). If the concentration is <0.1 N NaCl, the complex permittivity is equivalent to that of water. We use $\epsilon_s^*(\omega) - \sigma/j\omega\,\epsilon_o$ instead of $\epsilon_s^*(\omega)$ in Equation (3) where σ is the dc conductivity and ϵ_o is the dielectric constant *in vacuo.* The dc conductivity can also be estimated using pure water as the reference from the measurements of the reflected wave over a significantly long period. We employed "time windows" to identify the total dielectric spectrum. Depending on the sample, the longest time window or period was selected so that $R_s(t) - R_x(t)$ definitely reaches zero. Figure 1a and 1b shows $R_s(t) - R_x(t)$ of the allophane and kaolinite at the longest time window, respectively. Note that the kaolinite sample has the relaxation process at the lower-frequency region, compared with allophane. If t_1 is defined as the time when $R_s(t) - R_x(t)$ reaches zero, ρ in Equation (3) can be described by Equation (4) (Table 1).

Two sample cells with different d and γ_d were employed in this study. For accurate measurements in a frequency range >100 MHz, the shorter cell with d = 0.01 mm and γ_d = 0.13 mm was used. In the range below 1 GHz, a cell with d = 2.0 mm and γ_d = 4.54 mm was used. Time windows employed were 5 and 20 ns for the shorter cell and 50, 100, 200, 500 ns, 1, 2, 5, and 10 μs for the longer cell. By using these cells, even very small relaxation with a relaxation strength of the magnitude of 0.1 may be measured in the frequency region of concern (Umehara *et al.,* 1990). For the overlapping region of frequency between 100 MHz and 1 GHz, data obtained by the two cells were in agreement. Data accumulation was done with five repetitions for the complex permittivity. To obtain a high resolution of frequency, a narrow frequency interval of 0.05 on a logarithmic scale was used.

RESULTS

Dielectric-dispersion and absorption curves of moist kaolinite are shown in Figure 2. Two inflections are faintly observed in the dispersion curve near 100 kHz and 100 MHz (Figure 2a), but the corresponding relaxation peak cannot be distinguished from the absorption curve (Figure 2b). The absorption owing to dc conductivity is so large that the small relaxation peaks are not apparent. When the contribution of the dc conductivity is subtracted (Figure 3), the two relaxation peaks appear clearly around those frequency regions, as shown in Figure 3b. Thus, the total dispersion and absorption curves are described well by the sum of three relaxation processes as given by Equation (5) (Table 1). The parameters in Equation (5), determined by *least-squares,* are listed in Table 2. For montmorillonite, a similar relaxation model explains the total relaxation spectra satisfactorily as shown in Figure 4. The relaxation parameters identified are given in Table 2. The total dispersion and absorption curves for allophane and imogolite were described well by Equations (6) and (7), respectively (Table 1). The determined relaxation parameters are given in Table 2. These parameters based on the best fit explain the total relaxation spectra satisfactorily as shown in Figures 5 and 6 for allophane and imogolite, respectively.

https://doi.org/10.1346/CCMN.2000.0480110 Published online by Cambridge University Press

Table 1. List of equations.

$$\epsilon_x^* = \epsilon_x'(\omega) - j\epsilon_x''(\omega)$$

$$= \frac{c}{j\omega\gamma_d}\frac{\upsilon_0(\omega) - r_x(\omega)}{\upsilon_0(\omega) + r_x(\omega)}Z_x(\omega)\cot Z_x(\omega) \quad (1)$$

where

$$Z_x(\omega) = \left(\frac{\omega d}{c}\right)\epsilon_x^*(\omega)^{1/2}$$

$$\epsilon_s^*(\omega) = \epsilon_s'(\omega) - j\epsilon_s''(\omega)$$

$$= \frac{c}{j\omega\gamma_d}\frac{\upsilon_0(\omega) - r_s(\omega)}{\upsilon_0(\omega) + r_s(\omega)}Z_s(\omega)\cot Z_s(\omega) \quad (2)$$

where

$$Z_s(\omega) = \left(\frac{\omega d}{c}\right)\epsilon_s^*(\omega)^{1/2}$$

where the subscripts x and s refer to samples of unknown and known permittivities, respectively; $\epsilon'(\omega)$ and $\epsilon''(\omega)$ are functions that produce dispersion and absorption curves of complex permittivity, respectively; j represents an imaginary unit; d and γ_d are geometrical and effective electrical lengths of the coaxial sample cell, respectively; $\upsilon_0(\omega)$ is the Fourier transform of the incident pulse applied to the sample; $r(\omega)$ is that of the reflected pulse R(t); and c is the speed of propagation *in vacuo*. The term $Z(\omega)\cot Z(\omega)$ accounts for the multiple reflection in the sample section.

$$\epsilon_x^*(\omega) = \epsilon_s^*(\omega)\frac{1 + \{cf_s(\omega)/[j\omega\gamma_d\epsilon_s^*(\omega)]\}\rho(\omega)}{1 + \{[j\omega\gamma_d\epsilon_s^*(\omega)]/cf_s(\omega)\}\rho(\omega)}\frac{f_x(\omega)}{f_s(\omega)} \quad (3)$$

where

$$\rho(\omega) = \frac{r_s(\omega) - r_x(\omega)}{r_s(\omega) + r_x(\omega)} \qquad f_x(\omega) = Z_x(\omega)\cot Z_x(\omega),$$

$$f_s(\omega) = Z_s(\omega)\cot Z_s(\omega)$$

$$\rho(\omega) = \frac{\int_0^{t_l}[R_s(t) - R_x(t)]e^{-j\omega t}\,dt}{2\int_0^{t_l}[R_s(t)]e^{-j\omega t}\,dt - \int_0^{t_l}[R_s(t) - R_x(t)]e^{-j\omega t}\,dt} \quad (4)$$

$$\epsilon^*(\omega) = \epsilon_\infty + \frac{\Delta\epsilon_l}{(1 + j\omega\tau_l)^{\alpha_l}} + \frac{\Delta\epsilon_m}{1 + (j\omega\tau_m)^{\beta_m}} + \frac{\Delta\epsilon_h}{1 + (j\omega\tau_h)^{\beta_h}} \quad (5)$$

$$\epsilon^*(\omega) = \epsilon_\infty + \frac{\Delta\epsilon_l}{(1 + j\omega\tau_l)^{\alpha_l}} + \frac{\Delta\epsilon_m}{(1 + j\omega\tau_m)^{\alpha_m}} + \frac{\Delta\epsilon_h}{1 + (j\omega\tau_h)^{\beta_h}} \quad (6)$$

$$\epsilon^*(\omega) = \epsilon_\infty + \frac{\Delta\epsilon_l}{1 + j\omega\tau_l} + \frac{\Delta\epsilon_h}{1 + (j\omega\tau_h)^{\beta_h}} \quad (7)$$

where the subscripts l, m, and h refer to the relaxation process at low, intermediate, and high frequencies, respectively, ϵ_∞ is the dielectric constant extrapolated to $\omega = \infty$, $\Delta\epsilon$ is the relaxation strength, τ is the relaxation time, and α and β are the Cole-Davidson and Cole-Cole parameters (*e.g.*, Hill *et al.*, 1969) representing the distribution of relaxation times, respectively.

$$\tau_l = \frac{\epsilon_c'(n - 1) + \epsilon_s'}{4\pi\sigma_s} \quad (8)$$

where ϵ_c' and ϵ_s' are the dielectric constant of clay and solution, respectively; σ_s is dc conductivity and n is a shape factor.

Table 1. Continued.

$$\tau_l = \frac{r^2}{2u_l kT} \quad (9)$$

where

$$u_l = u_0\exp\left(\frac{-E}{kT}\right)$$

where r is the radius of a spherical particle or the half-length of a rod-shaped particle, u_0 is the sodium volocity per unit force in water, k is the Boltzmann constant, T is the absolute temperature, and E is the potential barrier for the migration.

$$\Delta\epsilon_l = \frac{9}{4}\frac{p}{\left(1 + \frac{p}{2}\right)^2}\frac{q^2 r\delta}{\epsilon_0 kT} \quad (10)$$

where p is the volume fraction of clay, q is the electronic charge unit, ϵ_0 is the dielectric constant of the vacuum and δ is the charge density.

DISCUSSION

Non-bound water

The values of the relaxation time τ_h for the process at high frequencies at 20 GHz are not dependent on

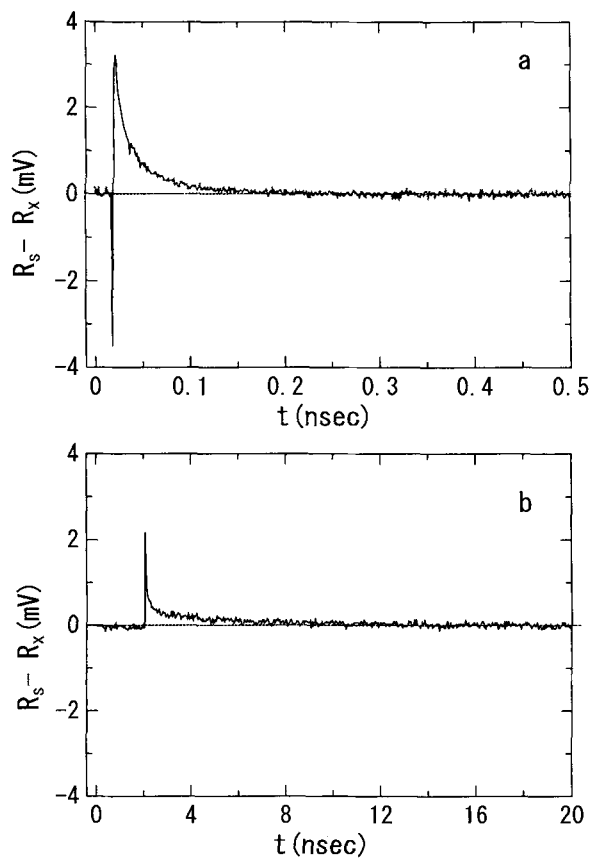

Figure 1. For a long-time range, the time-domain signal $R_s - R_x$ reaches zero for (a) allophane and (b) kaolinite.

https://doi.org/10.1346/CCMN.2000.0480110 Published online by Cambridge University Press

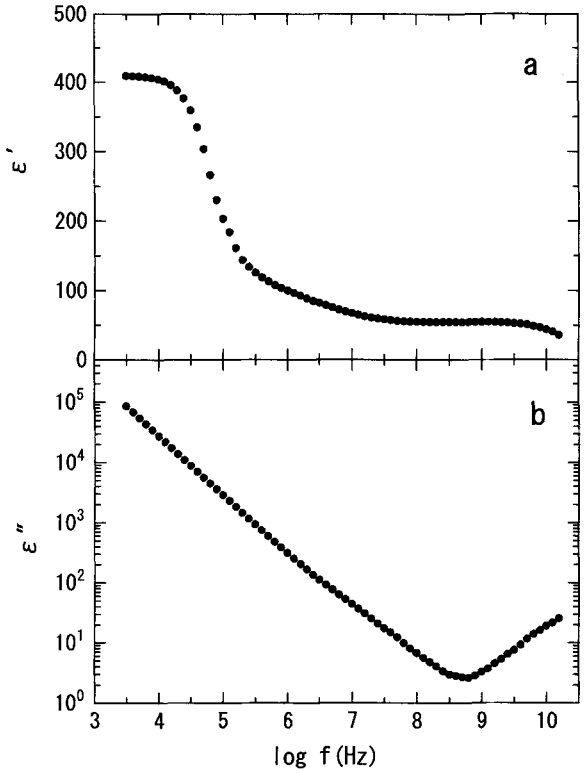

Figure 2. Experimental dielectric-dispersion (a) and absorption curves (b) for moist kaolinite, including the contribution of dc conductivity, f = frequency.

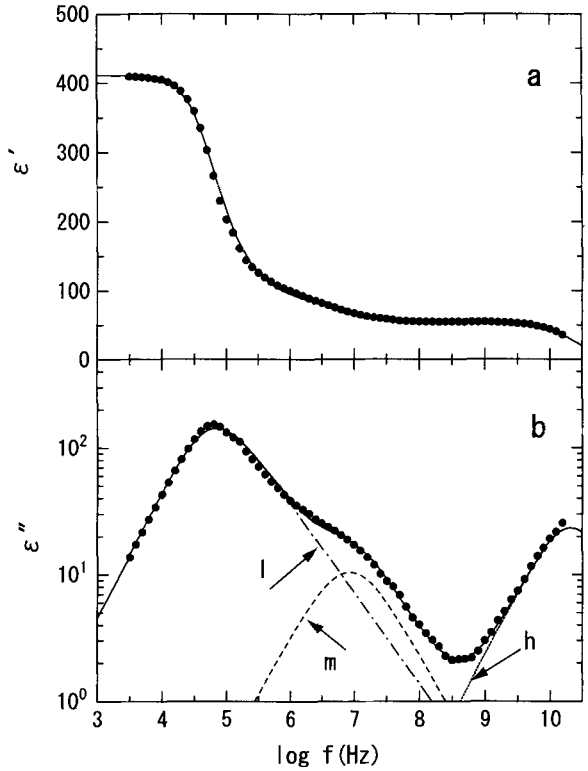

Figure 3. Dielectric-dispersion (a) and absorption (b) curves for moist kaolinite obtained after the contribution of dc conductivity is subtracted. ● reveals the observed data. "h", "m", and "l" refer to the high-, intermediate-, and low-frequency processes, respectively. Solid, dotted, broken, and chain lines show total, "h", "m", and "l" processes, respectively, calculated from Equation (5) by using relaxation parameters listed in Table 2. The mean errors over the frequency (f) of concern are within 3 and 7% for the dispersion and absorption curves, respectively.

the type of minerals studied here. These values range from 7.1 to 8.9 ps and compare favorably with previously determined values for pure water. For example, comparative values at 20 and 30°C are 9.2 and 7.2 ps, respectively (*e.g.,* Hill *et al.,* 1969). Thus, the process at high frequencies is caused by the reorientation of bulk-H_2O molecules. Sposito (1981) showed that the dielectric-relaxation time for bulk H_2O is related to the time constant for the reorientational motion of a single H_2O molecule, provided H_2O may be described as a rigid sphere that adheres to the interface. The dielectric-dispersion and absorption curves for all minerals except for montmorillonite are described well by the Cole-Cole representation (Ishida and Makino, 1999a, 1999b). Figure 7 illustrates the relationship between the relaxation strength $\Delta\epsilon_h$ and the water content, showing that the values of $\Delta\epsilon_h$ increase with an increase in water content.

Bound water

For imogolite, the low-frequency process near 10 MHz is caused by the orientation of bound H_2O on the imogolite surface, based on relaxation strength and time. The dielectric relaxation is a pure Debye contribution, which indicates that the contribution excludes the distribution of relaxation time, and thus interfacial polarization is not of interest in this study. If interfacial polarization occurred, the relaxation time is distributed as a result of inhomogeneous interactions of imogolite tubes. The value of τ_l, 22 ns, is 1000 times smaller than for pure ice (Hill *et al.,* 1969), whereas it is approximately ten times larger than that of bound H_2O in biological materials (*e.g.,* Mashimo *et al.,* 1987b).

The values of τ_l and α_l for allophane are similar to those for imogolite. The similarity in α_l implies that the distribution of relaxation times occurs within a small range. Because the allophane concentration is considerably greater than the concentration of imogolite, the content of bound H_2O or the relaxation strength for allophane is probably larger than for imogolite. Therefore, the process at low frequencies for allophane is attributed to the orientation of the bound H_2O. There probably is no other relaxation mechanism at intermediate frequencies for allophane except for the orientation of the bound H_2O, because only H_2O is active in dielectric relaxation in this frequency re-

https://doi.org/10.1346/CCMN.2000.0480110 Published online by Cambridge University Press

Table 2. Dielectric relaxation parameters in Equations (5)–(7) determined for the four moist samples.

Sample	log τ_i (s)	$\Delta \epsilon_i$	α_i	log τ_m (s)	$\Delta \epsilon_m$	α_m	β_m
Kaolinite	−5.52 ± 0.38	335.0 ± 21.4	0.71 ± 0.04	−7.72 ± 0.21	23.6 ± 1.6	1.00	0.92 ± 0.02
Montmorillonite	−6.58 ± 0.35	290.6 ± 22.4	0.73 ± 0.04	−8.06 ± 0.24	130.4 ± 9.3	1.00	0.81 ± 0.03
Allophane	−7.51 ± 0.21	24.6 ± 2.8	0.95 ± 0.03	−8.69 ± 0.18	5.6 ± 1.5	0.65 ± 0.03	1.00
Imogolite	−7.66 ± 0.24	7.2 ± 0.8	1.00				

gion. This result implies that two different structures of bound H_2O are present in allophane. The value of α_m is significantly smaller than that of α_i. Henmi (1991) showed that the thermal energy required to remove H_2O allows a distinction to be made between bound H_2O inside and outside of allophane spherules. The result of Henmi may support the two different bound-water structures.

For kaolinite and montmorillonite, the intermediate-frequency results are probably caused by bound H_2O, based on the values of τ_m, which are close to those for montmorillonite suspensions (Ishida and Makino, 1999b). However, these values are much smaller than those for Na-rich kaolinite complexes (Hall and Rose, 1978) and much larger than those for Na-rich montmorillonite (Mamy, 1968) at very low-water contents. The relaxation time at intermediate frequencies for kaolinite compares favorably with those for low frequencies for imogolite and allophane, whereas the relaxation time for montmorillonite is approximately twice as long. Based on differential heat measurements of water-vapor adsorption at low relative humidity, Iwata *et al.* (1989) stated that the affinity of H_2O for clay-like surfaces increases in the order: montmorillonite, kaolinite, and allophane. Regarding the relaxation time as a rough measure of the interaction of the mineral surface and the bound-H_2O molecule, the relaxation time obtained in this study is consistent with this order of affinity. The results obtained here also are consistent with Fripiat *et al.* (1965) relating to the mobility of H_2O molecules.

The bound H_2O for kaolinite and montmorillonite has a symmetric distribution of relaxation times, which is reflected by the Cole-Cole representation. The process occurring in the intermediate frequencies for allophane has an asymmetric distribution for the Cole-Davidson representation. The asymmetric distribution is generally observed in the chain motion of coiled polymers. This distribution arises from the correlation between segmental motion (*e.g.,* Harviliak and Negami, 1967). If the bound H_2O constructs a chain-like structure and the reorienting molecule correlates with neighboring molecules in the chain, the distribution will be asymmetric, similar to that of a chain polymer. If a "card-house" structure with edge-to-face contacts is formed in phyllosilicate minerals such as montmorillonite and kaolinite, then this structure may make the surface of the phyllosilicate energetically heterogeneous to produce a symmetric distribution of relaxation times. The dielectric curves of montmorillonite (Mamy, 1968; Calvet, 1975) and kaolinite (Hall and Rose, 1978) at very low-water contents are also described by the Cole-Cole representation. However, the values of α_m obtained in the present paper are about twice those obtained at these very low-water contents. The difference in the distribution pattern of relaxation times may indicate that the bound-H_2O structure on these mineral surfaces is formed in a dissimilar manner between the phyllosilicates and poorly crystalline phases.

Figure 8 shows the relaxation strength owing to bound H_2O relative to water content. This figure shows that the value of the relaxation strength for montmorillonite is remarkably higher than those for the other three phases. This anomalous property may provide additional understanding for the swelling mechanisms of montmorillonite. The relaxation strength is closely related to the number of bound-H_2O molecules and the square of the dipole moment. Bound-H_2O structure is reflected in values of the dipole moment. At present, it is difficult to relate the contributions of each. However, the relaxation strength may relate to a unique aspect about the bound-H_2O structure on the montmorillonite surface.

Interfacial polarization

Many workers (*e.g.,* Lockhart, 1980a, 1980b; Sen, 1981) observed large values for dielectric constants in the kHz range. Although these values may be related to polarizations of the double layer surrounding the charged clay particles (Dukhin, 1973), the detailed mechanism responsible for these large values is not understood. The mechanism involves electrochemical effects owing to the electrical properties of clay surfaces, as well as geometrical effects (Sen, 1981) owing to the shape of the particles.

The interfacial polarization may be related to processes occurring in the low-frequency regions for kaolinite and montmorillonite. Raythatha and Sen (1986) showed that the "tail" of the interfacial polarization persists in the MHz frequency range, as was observed here also. However, as discussed above, the relaxation process owing to the rotation of bound H_2O also appears in this frequency range. Although Raythatha and Sen considered that the contribution of bound H_2O to the total dielectric relaxation is too small to be important, the contribution is significant (see Figures 3 and 4). This observation results from the high precision of

Table 2. Extended.

log τ_h (s)	$\Delta \epsilon_h$	β_h	ϵ_∞
−11.12 ± 0.21	47.7 ± 1.9	0.98 ± 0.01	5.3 ± 0.6
−11.15 ± 0.17	59.1 ± 1.4	1.00 ± 0.00	4.2 ± 0.8
−11.07 ± 0.23	51.8 ± 2.5	0.97 ± 0.01	4.0 ± 0.7
−11.05 ± 0.12	69.5 ± 0.8	0.98 ± 0.01	5.2 ± 0.4

the dc estimate. Because data are insufficient to determine the interfacial-polarization mechanism quantitatively, we discuss the possible mechanisms in qualitative terms.

The Maxwell-Wagner effect commonly is used to explain the interfacial polarization on clays at low-water contents, for example, see Calvet (1975) and Helmy *et al.* (1988) for montmorilonite, or Goldsmith and Muir (1960) for kaolinite. We discuss the possibility of using the Maxwell-Wagner model in the form by Sillars (1936) for conducting spheroids in an insulating matrix. The relaxation time is given by Equation (8) (Table 1).

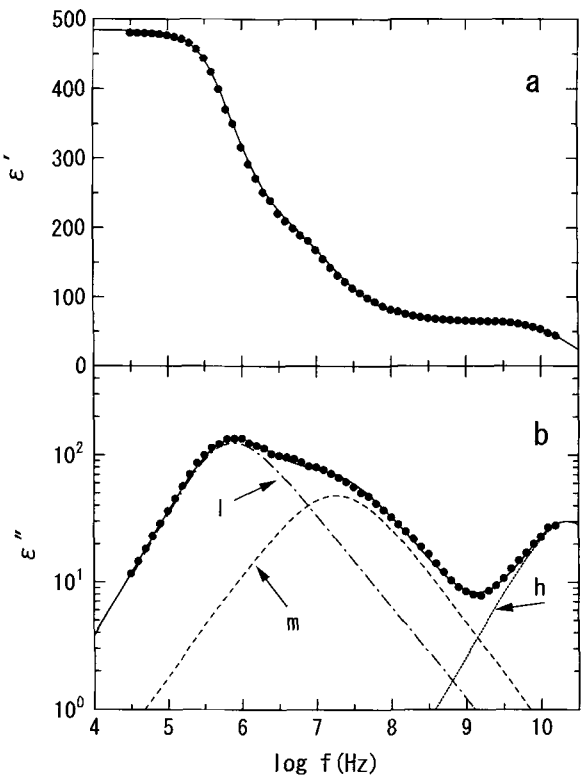

Figure 4. Dielectric-dispersion (a) and absorption (b) curves for moist montmorillonite obtained after the contribution of dc conductivity is subtracted. ● reveals the observed data. "h", "m", and "l" refer to the high-, intermediate-, and low-frequency processes, respectively. Solid, dotted, broken, and chain lines show total, "h", "m", and "l" processes, respectively, calculated from Equation (5) by using relaxation parameters listed in Table 2. The mean errors over the frequency (f) of concern are within 3 and 9% for the dispersion and absorption curves, respectively.

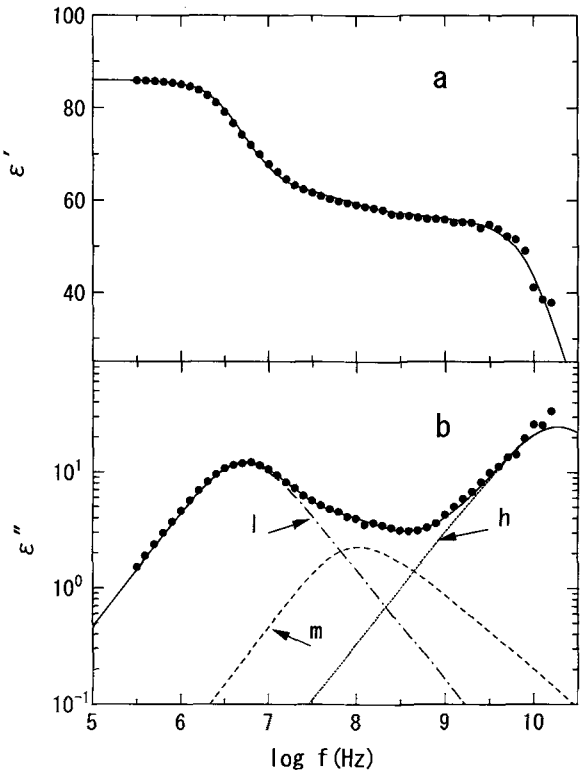

Figure 5. Dielectric-dispersion (a) and absorption (b) curves for moist allophane obtained after the contribution of dc conductivity is subtracted. ● reveals the observed data. "h", "m", and "l" refer to the high-, intermediate-, and low-frequency (f) processes, respectively. Solid, dotted, broken, and chain lines show total, "h", "m", and "l" processes, respectively, calculated from Equation (6) by using relaxation parameters listed in Table 2. The mean errors over the frequency of concern are within 2 and 5% for the dispersion and absorption curves, respectively.

If the relaxation time τ_l is assumed to be inversely proportional to the dc conductivity, the difference in τ_l between kaolinite and montmorillonite can be explained qualitatively by the Maxwell-Wagner effect or by the difference in dc conductivity. The dc conductivity is: kaolinite, 5.4 ± 0.5 mS/m; montmorillonite, 259.0 ± 11.3 mS/m; allophane, 58.2 ± 3.9 mS/m; imogolite, 11.0 ± 0.8 mS/m.

Another possible mechanism is the tangential migration (*i.e.*, surface-polarization effect) of counterions at the clay surface. Recently Ishida and Makino (1999b) performed dielectric measurements on montmorillonite suspensions under various pH conditions. They showed that the surface-polarization mechanism is a more appropriate model for the relaxation process observed at low frequency than the Maxwell-Wagner mechanism, based on the dependence of the relaxation times on dc conductivities. The relaxation time for the

https://doi.org/10.1346/CCMN.2000.0480110 Published online by Cambridge University Press

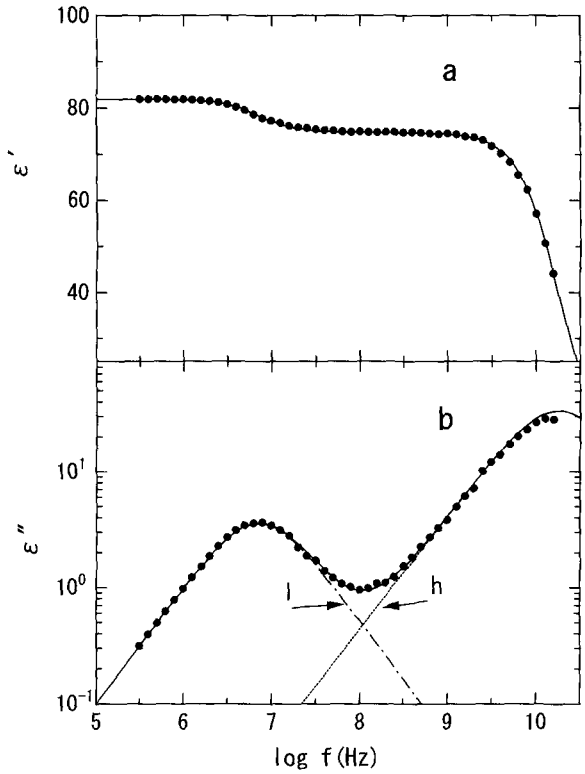

Figure 6. Dielectric-dispersion (a) and absorption (b) curves for moist imogolite obtained after the contribution of dc conductivity is subtracted. ● reveals the observed data. "h" and "l" refer to the high- and low-frequency processes, respectively. Solid, dotted, and chain lines show total, "h", and "l" processes, respectively, calculated from Equation (7) by using relaxation parameters listed in Table 2. The mean errors over the frequency (f) of concern are within 2 and 4% for the dispersion and absorption curves, respectively.

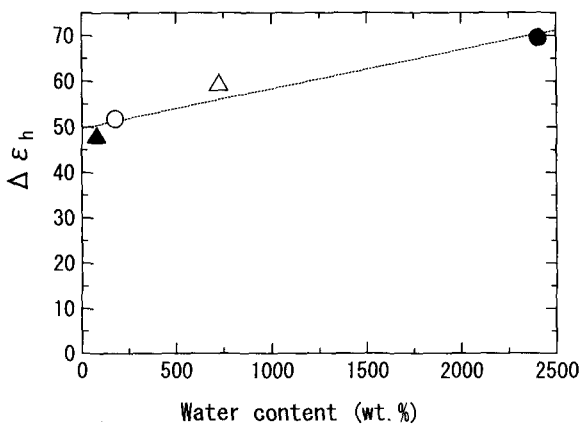

Figure 7. Dependence of $\Delta\epsilon_h$ on water content. ▲, kaolinite; △, montmorillonite; ○, allophane; ●, imogolite.

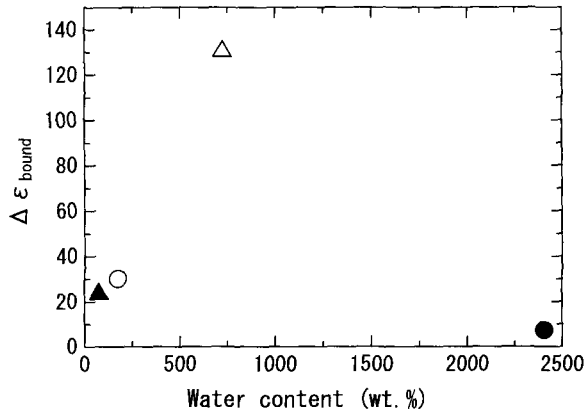

Figure 8. Dependence of relaxation strength owing to bound H_2O on water content. ▲, kaolinite; △, montmorillonite; ○, allophane; ●, imogolite.

counter-ion process is described (Schwarz, 1962) by Equation (9) of Table 1. Also, the relaxation strength (Schwarz, 1962) is given by Equation (10) of Table 1. The radius and charge density were estimated based on Ishida and Makino (1999b). The radii obtained are 0.092 and 0.031 μm for kaolinite and montmorillonite, respectively. The charge densities are 0.00071 and 0.0025 meq/m^2. Those values for montmorillonite are comparable with those in Ishida and Makino (1999b). The comparison in the values between kaolinite and montmorillonite indicates that the surface-polarization mechanism might be qualitatively reasonable (Lockhart, 1980a, 1980b). Therefore, we cannot determine which mechanism is responsible for the interfacial polarization under moist conditions.

However, the Maxwell-Wagner and surface-polarization effects cannot be general mechanisms responsible for interfacial polarization of all the mineral-water systems, because allophane and imogolite do not have a relaxation process despite both having dc conductivity comparable with that for kaolinite. The structure of the diffuse double layer is a key to the question of the general mechanism. A more detailed study of the interfacial polarization would provide useful information on the structure of the diffuse double layer. The information would contribute to the understanding of non-equilibrium electrical phenomena of clays or colloids (Dukhin, 1993).

ACKNOWLEDGMENTS

The authors dedicate this article to the late Professor Satoru Mashimo. We thank N. Miura for the technical development and support of the TDR system used. This study was partly supported by a Grant-in-Aid for scientific research from the Ministry of Education, Culture and Science, Japan (Registry No. 09660259).

REFERENCES

Calvet, R. (1975) Dielectric properties of montmorillonites saturated by bivalent cations. *Clays and Clay Minerals,* **23,** 257–265.

Carrington, A. and McLachlan, A.D. (1967) *Introduction to Magnetic Resonance.* Harper & Row, New York, 266 pp.

Cole, R.H. (1975a) Evaluation of dielectric behavior by time domain spectroscopy. 1. Dielectric response by real time analysis. *Journal of Physical Chemistry,* **79,** 1459–1468.

Cole, R.H. (1975b) Evaluation of dielectric behavior by time domain spectroscopy. 2. Complex permittivity. *Journal of Physical Chemistry,* **79,** 1469–1474.

Cole, R.H., Mashimo, S., and Winsor, P., IV. (1980) Evaluation of dielectric behavior by time domain spectroscopy. 3. Precision difference methods. *Journal of Physical Chemistry,* **84,** 786–793.

Dukhin, S.S. (1973) Dielectric properties of disperse systems. In *Surface and Colloid Science, Volume 3,* E. Matijevic, ed., Academic Press, New York, 83–165.

Dukhin, S.S. (1993) Non-equilibrium electric surface phenomena. *Advances in Colloid and Interface Science,* **44,** 1–134.

Fripiat, J.J., Jelli, A., Poncelet, G., and Andre, J. (1965) Thermodynamic properties of adsorbed water molecules and electrical conduction in montmorillonites and silicas. *Journal of Physical Chemistry,* **69,** 2185–2197.

Fukuzaki, M., Umehara, T., Kurita, D., Shioya, S., Haida, M., and Mashimo, M. (1992) Measurement of bound water in an aqueous DNA solution using nuclear magnetic resonance and time domain reflectometry. *Journal of Physical Chemistry,* **96,** 10087–10089.

Fukuzaki, M., Miura, N., Shinyashiki, N., Kurita, D., Shioya, S., Haida, M., and Mashimo, M. (1995) Comparison of water relaxation time in serum albumin solution using nuclear magnetic resonance and time domain reflectometry. *Journal of Physical Chemistry,* **99,** 431–435.

Goldsmith, B.J. and Muir, J. (1960) Surface ion effects in the dielectric properties of adsorbed water films. *Journal of Chemical Society, Faraday Transactions 1,* **56,** 1656–1661.

Hall, P.G. and Rose, M.A. (1978) Dielectric properties of water adsorbed by kaolinite clays. *Journal of Chemical Society, Faraday Transactions 1,* **74,** 1221–1233.

Havriliak, S. and Negami, S. (1967) A complex plane representation of dielectric and mechanical relaxation processes in some polymers. *Polymer,* **8,** 161–210.

Helmy, A.K., Santamaria, R.M., and Garcia, N.J. (1988) Dielectric behavior of montmorillonite discs. *Colloids and Surfaces,* **34,** 13–21.

Henmi, T. (1991) Idea and methodology on the study of amorphous clays. *Journal of Clay Science Society of Japan,* **31,** 75–81. (in Japanese).

Hertz, H.G. (1973) Nuclear magnetic relaxation spectroscopy. In *Water, A Comprehensive Treatise, Volume 3,* F. Frank, ed., Plenum Press, New York, 301–400.

Hill, N.E., Vaughan, W.E., Price, A.H., and Davies, M. (1969) *Dielectric Properties and Molecular Behaviour.* Van Nostrand Reinhold, London, 480 pp.

Hoekstra, P. and Doyle, W.T. (1971) Dielectric relaxation of surface adsorbed water. *Journal of Colloid and Interface Science,* **36,** 513–521.

Ishida, T. and Makino, T. (1999a) Microwave dielectric relaxation of bound water to silica, alumina, and silica-alumina gel suspensions. *Journal of Colloid and Interface Science,* **211,** 144–151.

Ishida, T. and Makino, T. (1999b) Effects of pH on dielectric relaxation of montmorillonite, allophane, and imogolite suspensions. *Journal of Colloid and Interface Science,* **211,** 152–161.

Iwata, S., Izumi, F., and Tsukamoto, A. (1989) Differential heat of water adsorption for montmorillonite, kaolinite and allophane. *Clay Minerals,* **24,** 505–512.

Jackson, M.L. (1979). *Soil Chemical Analysis-Advanced Course, 2nd edition.* M. L. Jackson, Madison, Wisconsin, 895 pp.

Lockhart, N.C. (1980a) Electrical properties and the surface characteristics and structure of clays. I. Swelling clays. *Journal of Colloid and Interface Science,* **74,** 509–519.

Lockhart, N.C. (1980b) Electrical properties and the surface characteristics and structure of clays. II. Kaolinite-a non-swelling clay. *Journal of Colloid and Interface Science,* **74,** 520–529.

Mamy, J. (1968) Recherches sur l'hydration de la montmorillonite: propriétés diélectriques et structure du film d'eau. *Annales Agronomiques,* **19,** 175–246.

Mashimo, S., Umehara, T., Ota, T., Kuwabara, S., Shinyashiki, N., and Yagihara, S. (1987a) Evaluation of complex permittivity of aqueous solution by time domain reflectometry. *Journal of Molecular Liquids,* **36,** 135–151.

Mashimo, S., Kuwabara, S., Yagihara, S., and Higasi, K. (1987b) Dielectric relaxation time and structure of bound water in biological materials. *Journal of Physical Chemistry,* **91,** 6337–6338.

Mashimo, S., Umehara, T., and Kuwabara, S. (1989) Dielectric study on dynamics and structure of water bound to DNA using a frequency range 10^7–10^{10} Hz. *Journal of Physical Chemistry,* **93,** 4963–4967.

Mehra, O.P. and Jackson, M.L. (1960) Iron oxide removal from soils and clays by a dithionite citrate system buffered with sodium bicarbonates. *Clays and Clay Minerals,* **7,** 317–327.

Miura, N., Asaka, N., Shinyashiki, N., and Mashimo, S. (1994) Microwave dielectric study on bound water of globule proteins in aqueous solution. *Biopolymers,* **34,** 357–364.

Miyauchi, N. and Aomine, S. (1966) Mineralogy of gel-like substance in the pumice bed in Kanuma and Kitakami districts. *Soil Science and Plant Nutrition,* **12,** 187–190.

Muraoka, M. (1951) Reports on Ibusuki clay produced from Kagoshima Prefectures. *Bulletin of the Geological Survey of Japan,* **2,** 74–84.

Raythatha, R. and Sen, P.N. (1986) Dielectric properties of clay suspensions in MHz to GHz range. *Journal of Colloid and Interface Science,* **109,** 301–309.

Schwarz, G. (1962) A theory of the low-frequency dielectric dispersion of colloidal particles in electrolyte solution. *Journal of Physical Chemistry,* **66,** 2636–2642.

Sen, P.N. (1981) Relation of certain geometrical features to the dielectric anomaly of rocks. *Geophysics,* **46,** 1714–1720.

Shinyashiki, N., Asaka N., Mashimo S., Yagihara S., and Sasaki N. (1990) Microwave dielectric study on hydration of moist collagen. *Biopolymers,* **29,** 1185–1191.

Sillars, R.W. (1936) The properties of a dielectric containing semiconducting particles of various shapes. *Proceedings of Royal Society of London A,* **166,** 378–394.

Sposito, G. (1981) Single-particle motions in liquid water. II. The hydrodynamic model. *Journal of Chemical Physics,* **74,** 6943–6949.

Sposito, G. and Prost, R. (1982) Structure of water adsorbed on smectites. *Chemical Reviews,* **82,** 553–573.

Sueno, J. and Nakaishi, K. (1992) Thixotropic behaviors of sodium and calcium montmorillonites at salt concentrations in the vicinity of 0.3 N. *Clay Science,* **8,** 349–353.

Umehara, T., Kuwabara, S., Mashimo, S., and Yagihara, S. (1990) Dielectric study on hydration of B-, A-, and Z-DNA. *Biopolymers,* **30,** 649–656.

Weiler, R.A. and Chaussidon, J. (1968) Surface conductivity and dielectrical properties of montmorillonite gels. *Clays and Clay Minerals,* **16,** 147–155.

Winsor, P., IV and Cole, R.H. (1982a) Dielectric properties of electrolyte solutions. 1. Sodium iodide in seven solvents at various temperatures. *Journal of Physical Chemistry,* **86,** 2486–2490.

Winsor, P., IV and Cole, R.H. (1982b) Dielectric properties of electrolyte solutions. 2. Alkali halides in methanol. *Journal of Physical Chemistry,* **86,** 2491–2494.

Yoshinaga, N. (1966) Chemical composition and some thermal data of eighteen allophanes from Ando soils and weathered pumices. *Soil Science and Plant Nutrition,* **12,** 47–54.

E-mail of corresponding author: ishida@ag.kagawa-u.ac.jp
(*Received 8 September 1998; accepted 21 July 1999; Ms. 98-111*)